Experimental studies of the magnetized friction force

Article *in* Physical Review E · July 2006

DOI: 10.1103/PHYSREVE.73.066503 · Source: PubMed

CITATIONS
16

READS
105

7 authors, including:

B. Galnander
European Spallation Source (ESS)
35 PUBLICATIONS **447** CITATIONS
SEE PROFILE

Vladimir N Litvinenko
Stony Brook University
438 PUBLICATIONS **5,689** CITATIONS
SEE PROFILE

Tor Lofnes
Uppsala University
31 PUBLICATIONS **148** CITATIONS
SEE PROFILE

A.O. Sidorin
Joint Institute for Nuclear Research
174 PUBLICATIONS **945** CITATIONS
SEE PROFILE

Experimental studies of the magnetized friction force

A. V. Fedotov,[1] B. Gålnander,[2] V. N. Litvinenko,[1] T. Lofnes,[2] A. Sidorin,[3] A. Smirnov,[3] and V. Ziemann[2]
[1]*Brookhaven National Laboratory, Upton, New York 11973, USA*
[2]*The Svedberg Laboratory, S-75121 Uppsala, Sweden*
[3]*JINR, Dubna, Russia*

(Received 23 December 2005; published 28 June 2006)

High-energy electron cooling, presently considered as an essential tool for several applications in high-energy and nuclear physics, requires an accurate description of the friction force which ions experience by passing through an electron beam. Present low-energy electron coolers can be used for a detailed study of the friction force. In addition, parameters of a low-energy cooler can be chosen in a manner to reproduce regimes expected in future high-energy operation. Here, we report a set of dedicated experiments in CELSIUS aimed at a detailed study of the magnetized friction force. Some results of the accurate comparison of experimental data with the friction force formulas are presented.

DOI: 10.1103/PhysRevE.73.066503 PACS number(s): 29.27.Bd

I. INTRODUCTION

Electron cooling [1] of heavy particle beams is used in a wide range of experiments in elementary-particle physics, nuclear physics, atomic physics, and other applications [2–4]. High-energy electron cooling (with relativistic parameter $\gamma \gg 1$) can open new possibilities in particle physics by producing high-quality high-density beams in colliders. However, the cooling times at high energy are much longer than the cooling times in present low-energy coolers. As a result, typical order of magnitude estimates of cooling times for high energy become insufficient. An accurate estimate of the cooling times requires the detailed description of Coulomb collisions in a strong magnetic field, a topic which is of great interest both for accelerator and plasma physics communities. Coulomb collisions in a magnetic field can be described by the friction force which ions experience when moving through the electron beam of the cooler. In this paper we discuss measurements of the longitudinal friction force (the component parallel to the magnetic field and the direction of propagation of the electron beam) for protons at injection energy (48 MeV) in CELSIUS [5,6].

The friction force as a function of various parameters has been measured before (see, for example, Refs. [2,7,8] and references therein). However, it was realized that in order to have an accurate description at the level needed for high-energy cooling predictions, the measurements should be specifically aimed towards such a goal. This requires not just a high precision of the measurements but also a well-controlled experiment where all needed parameters are carefully recorded. It also requires a careful optimization of the cooling process and minimization of various effects which may obscure the comparison with theory. For example, if the electron and the ion beam are not perfectly aligned the values of the friction force are significantly reduced, so that even the nonmagnetized friction force description might explain the measurements [9]. One needs to carefully minimize such effects in order for the measurements to be suitable for a detailed comparison with available theoretical models such as the recent numerical study of the magnetized friction force [10].

Here, we describe the measurements done in December 2004 and March 2005, which were performed as part of a collaboration between BNL and European laboratories working on high-energy cooling for the RHIC-II [11] and FAIR projects [12]. In addition to the well-controlled experiments with careful optimization of cooling, the parameters of the proton distribution during the measurements were recorded as well. We found that convoluting the single-particle formulas with the proton distribution function is essential for a correct comparison with measured data.

For standard operational parameters of the cooler the force was measured: (i) for various currents of the electron beam; (ii) for different alignment angles between electron and ion beams; (iii) for different strengths of the magnetic field errors in the cooling solenoid. In addition, standard parameters of the cooler were altered in order to explore effects that are essential for the understanding of high-energy magnetized cooling: (iv) description of Intrabeam Scattering (IBS) for non-Gaussian distributions which appears as a result of a slow cooling process; (v) various regimes of magnetization.

II. FRICTION FORCE MEASUREMENT

For low relative velocities between ions and electrons the longitudinal magnetized friction force increases linearly with velocity, reaching its maximum near the longitudinal velocity spread of the electron beam. In a realistic situation there are various effects which can contribute to the longitudinal velocity spread of the electron beam (see Sec. IV for discussions). An rms velocity spread in a realistic cooler environment is often referred to as an "effective velocity" (a notation which we use in this paper as well). For relative velocities higher than the effective velocity the force has a nonlinear dependence. In the linear region, the most accurate way of measurement is the phase-shift method. It uses a bunched ion beam and is based on measuring the phase difference between the rf system and the ion beam, resulting from the competition of the weak rf voltage and the longitudinal friction force. Using an accurate phase discriminator [13], one

TABLE I. Estimate of errors for $v_\parallel$.

Value	Error	Comment
C_r 81.76 m	±0.1%	circumference
η_p 0.783	±0.5%	from optics
Δf	±0.01%	frequency generator
$v_\parallel$	±0.5%	total error

can determine the cooling force acting on the ion of charge (Ze) via

$$F_\parallel = \frac{ZeU_{rf}\sin\Delta\phi_s}{L_c}, \tag{1}$$

where L_c is the length of the cooling solenoid, U_{rf} is the rf amplitude, and $\Delta\phi_s$ is the equilibrium phase difference between the ion beam and the rf cavity.

Typically, the relative velocity difference is introduced by changing the energy of the electron beam. However, changing the electron acceleration voltage is usually done with a rather large voltage step, which does not allow an accurate mapping near the force maximum and is hampered by the regulation of the high-voltage power supply. On the other hand, since this method employs bunched beams, changing the energy of the ion beam by changing the frequency of the rf cavity is more accurate. In our experiments, changing the rf frequency by a few Hz resulted in a very fine step in the relative velocity. A similar technique was used successfully before, for example, at IUCF [14].

A high precision in the measurements was obtained due to a combination of the two effects: (i) changing the rf frequency instead of the electron voltage step, and (ii) accurate measurements of the phase difference using the phase discriminator. An estimate of errors in our measurements is summarized in Tables I and II.

In the figures shown in this paper we present the raw measurements of the relative phase shift $\Delta\phi$ vs the frequency change Δf (10-Hz steps of 1129 kHz) for the protons at 48 MeV, which are converted to the plots of the drag force $F_\parallel$ vs $v_\parallel$, respectively, using Eqs. (1) and (2), and parameters in Tables I and II. The relative velocity between ions and electrons in the co-moving frame $v_\parallel$ is plotted in units of 10^4 m/s, and is calculated using

$$v_\parallel = \frac{\beta c}{\eta_p}\frac{\Delta f}{f_0} = \frac{C_r}{\eta_p}\frac{\Delta f}{h}, \tag{2}$$

where c is the velocity of light, β is the relativistic factor, η_p is the slip factor, Δf and f_0 are the frequency shift and rf frequency, C_r is the ring circumference and h is harmonic number of the Schottky signal ($h=1$ in our experiments). The uncertainty in determining $v_\parallel$ is relatively small, and is dominated by the accuracy in the value of the slip factor η_p, which is about 0.5%. The uncertainty in the values of $F_\parallel$ is dominated by our knowledge of the effective cooler length and the true value of the rf voltage. Using two different techniques to measure the rf amplitude (a probe in the cavity and the synchrotron frequency), the accuracy of U_{rf} was found to be about ±7%. A total relative error of the measurements of the longitudinal friction force is estimated to be about ±12% (see Table II), which is sufficient for a detailed comparison with available theoretical models.

TABLE II. Estimate of errors for $F_\parallel$.

Value	Error	Comment
U_{rf} 10.2 V	±7%	measurement
$\Delta\phi$	±1%	phase discriminator
L_c 2.50 m	±10%	cooler length
$F_\parallel$	±12%	total error

TABLE III. Parameters of electron cooler for standard settings.

Magnetic field B	0.1 T
Cooler length	2.5 m
Electron beam radius	0.01 m
Transverse rms velocity spread of electrons	1.4×10^5 m/s
Major contributors to longitudinal rms velocity spread:	
longitudinal-longitudinal relaxation	$\sim3-5\times10^3$ m/s
high voltage power supply ripple	5.2×10^3 m/s
magnetic field errors	$\sim10^4$ m/s

III. OBJECTIVE AND EXPERIMENTAL DATA

Our main goal was to collect data with an uncertainty of just a few percent (see Tables I and II). In all the experiments, the proton and electron beam were first perfectly aligned by minimizing the spread of the beam profiles on the H^0 detector located outside of the cooling section. The H^0 monitor is a silicon-strip detector situated 9 m from the cooler [6]. A tilt angle of 1 mrad thus corresponds to a movement of 9 mm at the H^0 detector. The resolution of the H^0 detector is 1 mm, giving a resolution of about 0.1 mrad for the tilt angle. If the electron and ion beams are not carefully aligned, the values of the friction force are significantly reduced and the interpretation of the friction force observed can be misleading.

Friction force measurements were done with a low-current (~50 μA) precooled proton beam with a typical rms size of 0.8 mm and a very small momentum spread (see Sec. IV C), making the effect of dispersion negligible. For such a well-aligned beam of small size the effect of a nonuniformity of electron density across the proton beam is also negligible.

The parameters of the electron cooler for standard settings are summarized in Table III. The estimates for the rms transverse and longitudinal velocity spread of the electrons in the beam frame are also given for completeness. Details about various contributions to the longitudinal velocity spread are discussed in Sec. IV.

Note that the analysis presented in this paper does not depend on the uncertainty of these estimates, as explained in Sec. IV. Instead, we use the measured values of the velocity

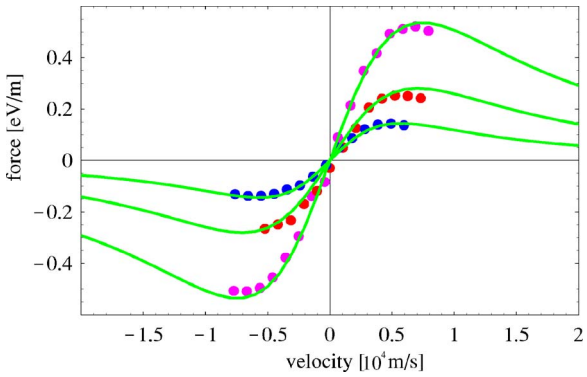

FIG. 1. (Color online) Longitudinal friction force in [eV/m] vs velocity [$\times 10^4$ m/s] for three currents of electron beam. Measured data: 250 (pink dots, upper curve), 100 (red dots, middle curve), and 50 (blue color) mA (B=0.1 T).

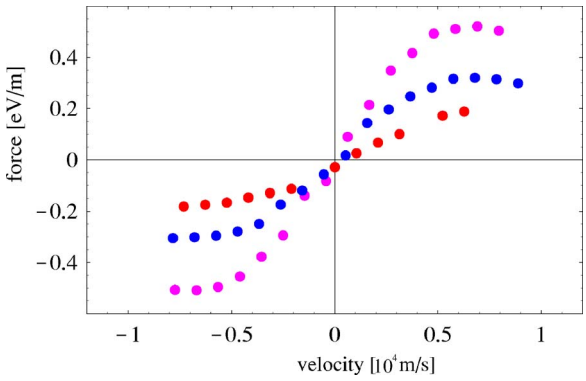

FIG. 2. (Color online) Longitudinal friction force in [eV/m] vs velocity [$\times 10^4$ m/s] for a misalignment angle between the beams in the horizontal direction: 0 (pink, upper curve), 0.4 (blue, middle curve), 0.8 (red) mrad (B=0.1 T, I_e=250 mA).

corresponding to the force maximum. The location of the force maximum (and thus the effective velocity) was recorded using the following technique. The derivative of the force changes its sign near the force maximum (see Fig. 1), resulting in large synchrotron oscillations for the relative velocities in the nonlinear part of the force [14]. The onset of such oscillations was recorded and provides accurate information about the relative velocity corresponding to the force maximum. The effective velocity can then be used in an analysis of experimental data, as shown in Sec. IV C.

(1) *Current dependence*. In the first experiment, the force was measured for various currents of the electron beam. For a typical settings of magnetic field B=0.1–0.12 T, the force curves were recorded for electron currents in the range of 20–500 mA. An example of the force measured for the electron currents of 250, 100, and 50 mA (B=0.1 T) is shown in Fig. 1. The data obtained allow one to study the scaling of the force with the current and intensity-dependent contributions to an effective velocity of the electrons. Moreover, it allows to determine the numerical coefficient in front of the friction force expression (see Sec. IV for details).

(2) *Alignment between beams*. In the second experiment, we explored the dependence of the effective velocity on the alignment angle between the ion and electron beam. A tilt angle introduces a significant contribution to the transverse component of the relative velocity in a controlled way and reduces the uncertainty in the estimated value of an effective velocity when comparing experimental data with models. The friction force was systematically measured for several horizontal and vertical tilt angles from 0.2 to 0.8 mrad in both negative and positive directions. The angle values were calibrated both with beam position monitors (BPMs) and the H^0 monitor. An example of the force measured for three tilt angles in the positive horizontal direction is shown in Fig. 2.

(3) *Transient cooling*. The goal of the third experiment was to study simultaneous effects due to electron cooling and intrabeam scattering (IBS) before the equilibrium parameters are reached. In a typical low-energy cooler, the electron cooling is so fast that one observes the rapid cooling of the ion beam profile as a whole. At high-energy with much slower cooling speed, one may observe the slow formation of a dense beam core with pronounced beam tails. For an accurate description of the luminosity gain for such distributions it becomes critical to have an accurate treatment of intrabeam scattering for non-Gaussian distributions. Recently, some models were developed in an attempt to describe this process [15–17]. In this experiment, the strength of the electron cooling was specifically reduced in order to capture such transient profiles of the ion beam.

In the longitudinal direction, the recorded bunch profile shows the formation of a core with a subsequent cooling of the large amplitudes, as shown in Fig. 3. The formation of non-Gaussian distributions is clearly observed. In the transverse direction, the transient evolution of the horizontal profiles was recorded with the magnesium jet profile monitor, which also showed formation of a dense core. These data will be used to improve models for the evolution of the beam distribution under the joint influence of IBS and electron cooling.

(4) *Different regimes of magnetization*. The fourth experiment was devoted to studying various degrees of magnetization. In a strong magnetic field, the electron dynamics in the transverse direction is effectively frozen, which, together

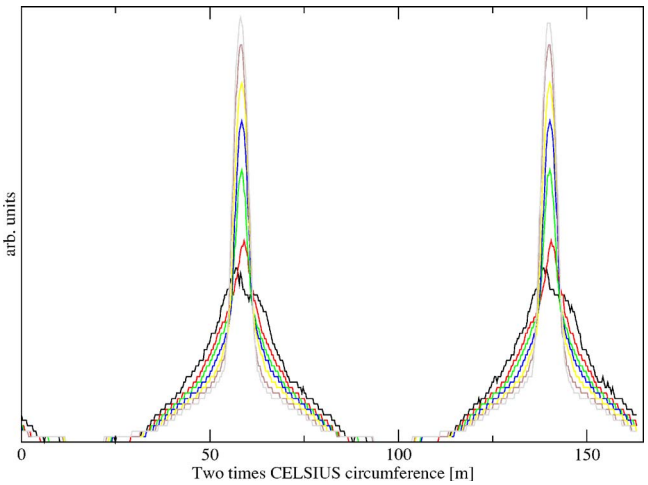

FIG. 3. (Color online) Longitudinal profiles of the proton beam for electron current I_e=20 mA and proton current I_p=0.6 mA, shown with time steps of 0.75 s.

with the flattened velocity distribution of the electrons, results in very fast cooling. As a result, for the magnetized component of the friction force there is only a weak logarithmic dependence on both the magnetic field and the transverse velocity spread of the electrons. It enters in the friction force expression through the Larmor radius under the Coulomb logarithm, appearing in the description of cooling based on binary collisions. However, if the maximum impact parameter in the magnetized collisions is not large compared to the Larmor circle one may encounter a strong nonlogarithmic dependence on both the magnetic field and the transverse velocity of the electrons if the parametrization of the friction force from Ref. [18] is used:

$$F = C\frac{4\pi n_e Z^2 e^4}{m_e}\frac{V}{(V^2+\Delta_{eff}^2)^{3/2}}L_M, \tag{3}$$

where V is the relative ion velocity, Δ_{eff} is the longitudinal effective velocity spread of the electrons. The magnetized Coulomb logarithm is defined as $L_M=\ln(\rho_{max}/\rho_L+1)$ with ρ_{max} being the maximum impact parameter in binary ion-electron collisions, and ρ_L being the Larmor radius, n_e and m_e are the density and mass of electrons, and C is some numeric coefficient. The value of this numeric coefficient C is discussed in Sec. IV.

For the purpose of the experiment discussed in this paragraph we are concerned only with the parametric dependence on the magnetic field in Eq. (3), which enters through the Larmor radius $\rho_L=m_e\Delta_{e\perp}/eB$, where $\Delta_{e\perp}$ is the transverse rms velocity spread of the electron distribution. If the maximum impact parameter in magnetized collisions is not large compared to the Larmor circle there is a possibility of a nonlogarithmic dependence on both the magnetic field and the transverse velocity of electrons. In such a case with $\alpha=\rho_{max}/r_L<1$ one can replace $\ln(\alpha+1)$ by α. As a result, the force has a linear dependence on the magnetic field and the transverse velocity of electrons which leads to a strong reduction in its absolute value.

We investigate this by measuring the friction force for various values of α. The values of α were controlled by changing the current of the electron beam (which changes the maximum impact parameter ρ_{max}) and the strength of the magnetic field (which changes ρ_L). As an example, the force measured for the values of $\alpha=1.3$ ($B=0.12$ T), $\alpha=1.0$ ($B=0.08$ T), $\alpha=0.9$ ($B=0.06$ T), $\alpha=0.8$ ($B=0.05$ T) (calculated based on the measured effective velocity) with $I_e=300$ mA is shown in Fig. 4.

(5) *Effect of solenoid errors*. In the fifth experiment, we explored the effects of solenoid errors which is not taken into account by most theoretical estimates. Such errors can, however, significantly decrease the strength of the force. The solenoid in the electron cooler in CELSIUS [6] contains embedded correctors to straighten the magnetic field lines. Several measurements of the friction force curve were performed with the correctors switched on and off. The data are presently being compared with numerical simulations using the VORPAL code [22], which calculates the friction force from first principles. An example of such a measurement for an electron current of $I_e=100$ mA is shown in Fig. 5 with the correctors switched on (blue dots) and off (red dots). The force is significantly reduced for larger perturbations of the magnetic field lines (correctors off). The measurements of the magnetic field errors in the CELSIUS cooler [6] report an rms angular spread as large as 1 mrad without correctors and less than 0.1 mrad with corrections [23]. Unfortunately, for this specific experiment, we did not have full control of the solenoid imperfections and just performed measurements with correctors either switched on or off. However, because these measurements were repeated for various electron beam currents they enable us to explore the relative contributions of the errors to the effective velocity of electrons (see Sec. IV A for more details).

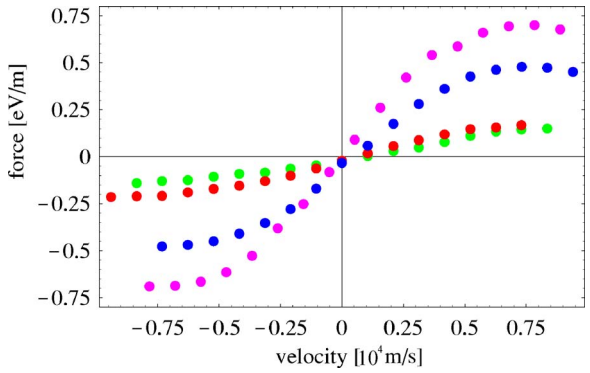

FIG. 4. (Color online) Longitudinal friction force in [eV/m] vs velocity [$\times 10^4$ m/s] for different magnetic fields with parameter $\alpha=1.3$ (pink dots, upper curve), 1.0 (blue), 0.9 (red), 0.8 (green, lower curve) from top to bottom, respectively.

For completeness and for future reference, we summarize below the parameters of the cooler for which the force curves measured were found to be of sufficient precision for an accurate comparison with available theoretical models and simulations.

For a perfectly aligned beam the curves were measured for $B=0.12$ T (electron current $I_e=500,300,100,50$ mA), $B=0.1$ T ($I_e=500,250,100,50,20$ mA), $B=0.08$ T ($I_e=500,300,100$ mA), $B=0.06$ T ($I_e=500,300,100$ mA), $B=0.05$ T ($I_e=500,300,100$ mA), $B=0.04$ T ($I_e=500,300$ mA), $B=0.03$ T ($I_e=300,100,50$ mA).

To explore the dependence on the nonstraightness of magnetic field lines, the measurements were also done with cor-

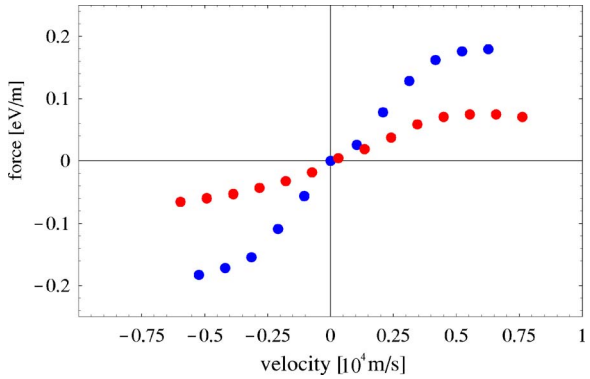

FIG. 5. (Color online) Longitudinal friction force in [eV/m] vs velocity [$\times 10^4$ m/s] with correctors on (blue dots, upper curve) and off (red dots) for $I_e=100$ mA and $B=0.06$ T.

rectors turned off for $I_e=500$ mA ($B=0.1, 0.04$ T), $I_e=300$ mA ($B=0.05, 0.04$ T), $I_e=100$ mA ($B=0.06, 0.03$ T).

To explore the dependence on the tilt angle between the proton and electron beams, the force was measured for $B=0.1$ T, $I_e=250$ mA for the horizontal tilt angles of $\theta_x=0$, 0.2, 0.4, 0.8, −0.2, −0.4, −0.8 mrad and for the angles in the vertical directions of $\theta_y=0$, 0.2, 0.4, 0.8, −0.2, −0.4, −0.8 mrad.

IV. FRICTION FORCE AND COMPARISON WITH THEORY

In this section comparison of the data with theory is discussed. However, the analysis is limited to a discussion of the fitting procedure and to some insights gained in our studies. Furthermore, only data from the first experiment are used in this section. In this experiment the friction force curves were recorded as a function of electron beam current for typical settings of the magnetic field with perfectly aligned beams (see Sec. III). An analysis of the other experiments, described in Sec. III, will be reported later.

A. Effective temperatures of the electron beam

Obtaining precise measurements of the friction force is not necessarily sufficient for a comparison of experimental data with theoretical models or for the benchmarking of numerical simulations. The main difficulty is typically associated with an uncertainty about the parameters of the electron beam, especially the transverse and longitudinal temperatures.

In our case, the transverse temperature and radius of the electron beam are taken to be $T_\perp=0.12$ eV (limit set by the cathode temperature) and $a_e=10$ mm, respectively. Extensive studies of the electron beam properties during the design and commissioning stage of the CELSIUS cooler and its electron gun showed that an uncertainty in these values is negligible [5,6] when operating at relatively low electron energies of 26 keV.

The CELSIUS electron gun adiabatically accelerates the electrons such that at low energies, between 10 and 50 keV, only a relatively weak magnetic field is needed to keep the transverse temperature of the electrons at a level of 0.1 eV. At higher energies, it is necessary to increase the magnetic field to 0.15 T [5], although with correction coils such an increase in electron temperature can be held at a very low level [6].

In most of our measurements at 26 keV energy of the electrons the excitation of the magnetic field values was $B=0.1-0.12$ T. For the case of the magnetized cooling (discussed in this paper) the transverse temperature is effectively suppressed by the magnetic field, and the uncertainty in its value contributes to the friction force only logarithmically. Note that an influence of the transverse temperature on the value of the magnetized force becomes significant only in our special experiment number 4 (see Sec. III), where standard parameters were intentionally altered to create such a dependence in order to study a transition from good to bad magnetization. But even in this special case when the magnetic field values were lowered, significant change in the electron beam parameters, for relatively low current ≤ 300 mA, is not expected [5,6]. Note also that the friction force measurements were done on a precooled proton beam with a typical rms size of 0.8 mm and very small momentum spread. For such well-aligned beams of a small size the effect of a nonuniformity of electron density across the proton beam is negligible.

During magnetic field measurements [6] of the cooler with correction coils the uncertainty in the magnetic field values was found to be very small. For example, for fields larger than 0.1 T the differences did not exceed 0.2 mT anywhere from the gun cathode to the end of the drift tube. This means that the radius of the electron beam in the cooling section is well determined by the emitting surface of the gun cathode.

There are many effects which may contribute to the longitudinal temperature (rms velocity spread) and determining the effective velocity spread is critical if one wants to estimate the location of the maximum of the longitudinal component of the friction force. Below we summarize major contributions to the effective velocity for our experiments. They include the ripple of the high-voltage power supply, the magnetic field errors, the intrabeam scattering within the electron beam, and the space-charge depression.

A significant contribution to the effective velocity spread, especially for low densities of the electron beam when the intensity-driven contributions are negligible, comes from the high voltage power supply ripple. In our case, it was measured to be about 3 V rms at 26 kV voltage, which gives a contribution to the rms longitudinal velocity spread v_{ripple} in the beam frame of around 5200 m/s.

Additional contribution may appear from the nonstraightness of the magnetic field lines. An estimate of the rms angular error, based on measurements [6,23], shows that it is about 0.1 mrad (with correctors), which corresponds to an rms velocity spread v_{err} of 10 000 m/s. Without the correctors the rms angular error is about 1 mrad.

One of the possible intensity-dependent contributions is, for example, the "longitudinal-longitudinal" relaxation. Before acceleration the electrons have kinetic energy (given by the temperature of the cathode) plus potential energy which results from the Coulomb field of the surrounding electrons. However, acceleration leads to a reduction of the kinetic energy in the beam frame according to $T_\parallel=T_c^2/(2W)$, where W is the kinetic energy of electrons, but the potential energy does not change. Under the assumption that acceleration is much faster than the characteristic interaction time between the electrons (on the order of the plasma frequency) the increase in the longitudinal energy spread can be estimated by an average electrostatic potential energy ($\sim e^2 n_e^{1/3}$ [7,8], where e and n_e is electron charge and density, respectively). For typical parameters of our experiments, an rms velocity spread v_{lon} due to such "longitudinal-longitudinal" relaxation is in the range from 3300 to 4900 m/s for the current of the electron beam from $I_e=50$ and $I_e=500$ mA, respectively.

Another intensity dependent contribution comes from the space charge of the electron beam which results in the drift of the electrons in the crossed electric field of the electron

beam and the longitudinal magnetic field of the cooler. Such a drift velocity v_d has a linear dependence on the beam current and is inversely proportional to the strength of the magnetic field. Other intensity-dependent contributions can be assumed to be negligible for a case of well-aligned beams.

Intrabeam scattering within the electron beam leads to "transverse-longitudinal" relaxation of the temperatures, which may significantly increase the longitudinal velocity spread. In a strong magnetic field such a relaxation is strongly suppressed [7,8]. Even for low values of the magnetic field used in our experiments we find the contribution of this effect negligible.

To reduce the uncertainty resulting from an estimate of the longitudinal velocity spread, we performed a parametric study of various parameters, which allows one to identify the relative contribution of each of the effect to the effective velocity of the electrons. For example, the friction force dependence on the current was measured for various strengths of the magnetic field, as well as with a different contribution from the magnetic field errors. In addition, in one of the experiments, the friction force was measured with carefully calibrated misalignments of the beams, which produced large values of an effective spread in a controlled way (see Sec. III).

Note that for the analysis reported in this paper (Sec. IV C), we do not use any estimate of an rms longitudinal velocity spread of the electrons. Instead, we use measured values of an effective velocity corresponding to the location of the friction force maximum which was recorded by an onset of the large-amplitude oscillations [14], as described in Sec. III. The use of the measured value of the total effective velocity as a known parameter may be more useful for the benchmarking of available models and simulations rather than an estimate of an effective velocity.

B. Fitting with a single-particle expression

In our fitting procedure, we use a parametric representation a single-particle friction force in Eq. (3). Note that such a representation also agrees with an analytic expression for the magnetized friction force in the linear region [19], which is the region of relative velocities discussed in this paper. A numeric coefficient $C=1/\pi$ was suggested by Parkhomchuk in Ref. [18]. It was obtained as a result of a direct fit of a measured average of the friction force for an ion distribution with a spread of the longitudinal and transverse velocity components. However, Parkhomchuk's formula [Eq. (3) with $C=1/\pi$] is generally presented and interpreted as being relevant to individual ions. For the linear part of the force the analytically derived coefficient for an individual ion is $C=1/(\sqrt{2}\pi)$, as reported by Derbenev and Skrinsky in Ref. [19]. Note that a known difference between Derbenev-Skrinsky asymptotics [19] and Parkhomchuk's empirical expression occurs only for large relative velocities $V \gg \Delta_{eff}$. Such a region of the velocities is not covered by the data reported in this paper. Recently, direct numerical simulations were performed, which helped to resolve various disagreements between the formulas [10].

In Fig. 6 one can see that for the electron currents of 50 (blue; lower curve), 100 (red), and 250 (pink) mA the curves

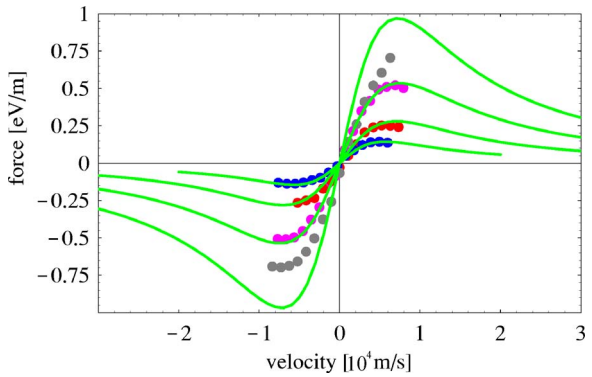

FIG. 6. (Color online) Longitudinal friction force in [eV/m] vs velocity [$\times 10^4$ m/s] for electron currents of 50 (blue, lowest set of data), 100 (red), 250 (pink), 500 mA (black, highest set of data) and a magnetic field in the cooling solenoid $B=0.1$ T.

based on Eq. (3) go nicely through the measured data points, although the resulting fitted value of the effective velocity Δ_{eff} has a weak dependence on the current. For a high electron current (500 mA), the experimental data are significantly lower than the curve utilizing the effective velocity determined from the low current data.

The high current data clearly shows that the effective velocity is completely dominated by intensity-dependent contributions. For example, for the set of the data with 500 mA ($B=0.1$ T) and measured parameters of the proton distribution the resulting drift velocity v_d is around 7400 m/s (calculated at an rms radius of cooled proton beam and an assumption that the electron beam is unneutralized). We can take this into account by adding an extra term to the effective velocity. This results in the solid curve shown in Fig. 7 that is based on Eq. (3).

A weak dependence of an effective velocity Δ_{eff} on the current in Fig. 6 appears close to the $n_e^{1/6}$ dependence which is an expected scaling if the effective velocity is completely determined by the longitudinal-longitudinal relaxation v_{lon} with all other contributions being negligible. The values of Δ_{eff} needed for a good fit of the data, in Figs. 6 and 7, are 6200, 8200, and 10 000 m/s (in the beam frame) for the currents $I_e=50$, 250, 500 mA, respectively.

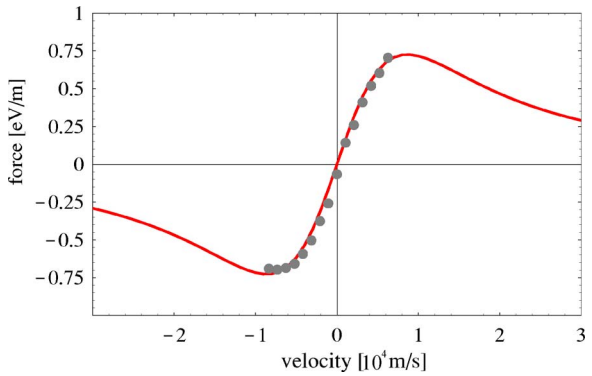

FIG. 7. (Color online) Measured friction force (points) in [eV/m] vs velocity [$\times 10^4$ m/s] for an electron current of 500 mA ($B=0.1$ T) and fitted curve based on Eq. (3) with an additional contribution to the effective velocity from the space charge of the electron beam.

However, for an accurate estimate, one should take into account other possible contributions to the velocity spread as well. For low currents such a direct contribution, in our case, comes from the power supply ripple and is estimated to be $v_{ripple}=5200$ m/s. For high currents, the space-charge contribution may become essential, which is estimated to be $v_d=3700$ and 7400 m/s for the currents of $I_e=250$ and 500 mA. Although an effect from the nonstraightness of the magnetic field lines on the location of the friction force maximum is clearly observed (see Fig. 5), its contribution to Δ_{eff} appears to be not as trivial as from other sources, and will be investigated with the VORPAL code [22].

In general, trying to identify the contribution of each of the effects to the effective velocity may have a relatively large uncertainty, apart from the cases where the effective velocity is clearly dominated by a single contribution (although it may be attempted with a help of a complete scan of the parameters, as the one reported in this paper). As a result, using the measured value for the force maximum and the corresponding effective velocity as a known parameter may be more valuable for the benchmarking of various models and simulations.

C. Averaging over ion distribution

In the previous section, the expression in Eq. (3) was directly fitted to experimental data. However, the precooled proton beam, with which the friction force measurements are made, has some finite values of an rms emittance and momentum spread. In order to determine an accurate numerical coefficient in the expression of the single-particle force by comparison with the measured data, one needs to convolute the single-particle expressions over the proton distribution.

The convolution over the proton distribution can be done according to

$$F = C\frac{4\pi Z^2 e^4 n_e}{m\sqrt{2\pi}\Delta_\perp^2\Delta_\parallel}\int_{-\infty}^{\infty}\frac{v_\parallel L_M(v_\parallel, v_\perp, \Delta_{eff})}{(v_\perp^2+v_\parallel^2+\Delta_{eff}^2)^{3/2}} \times \exp\left(-\frac{v_\perp^2}{2\Delta_\perp^2}-\frac{(v_\parallel-v_0)^2}{2\Delta_\parallel^2}\right) v_\perp dv_\perp dv_\parallel, \qquad (4)$$

where $\Delta_\parallel$ and $\Delta_\perp$ are measured rms velocities of the proton distribution, and the integrals are performed over the transverse $v_\perp$ and longitudinal $v_\parallel$ velocities of the protons.

In our experiments, the transverse distribution of the proton beam was measured using the Magnesium jet profile monitor. To get information about the longitudinal rms velocity spread, the longitudinal profiles were also measured. If the beam is longitudinally emittance dominated then the rms bunch length and the momentum spread are directly related, and by measuring bunch length one determines the values for the momentum spread. However, as a result of cooling, the beam may become longitudinally space-charge dominated, as it was brought to our attention by Nagaitsev [20,21]. In such a case, the actual momentum spread is much smaller than found from the relation between the bunch length and the momentum spread. For our experiments, we find that the cooled proton beam was longitudinally space-charge dominated even for a very small proton current of 50 μA. The bunch length measured scales as the third root of the proton beam current, as expected for the space-charge dominated beam [20]. Also, recorded longitudinal profiles are parabolic rather than Gaussian. For our experiments, the rms momentum spread determined from the measured bunch length is already small (around 5×10^{-5}). Taking into account that the actual momentum spread of such a longitudinally space-charge dominated beam is even smaller [21], we can assume that averaging in Eq. (4) is done essentially over the transverse ion distribution. Such an averaging with a negligible longitudinal momentum spread was used for the results presented in Figs. 8 and 9. For the data shown in Figs. 8 and 9, measured parameters of the proton distribution are the following: transverse full width at half maximum $\approx$2 mm, rms $dp/p=5.3\times10^{-5}$ (determined from the bunch length, actual momentum spread is expected to be much smaller [21]), $I_e=300$ mA, $B=0.12$ T. The beta functions in the cooler and in the magnesium jet location (transverse profiles) are 10 and 10.5 m, respectively.

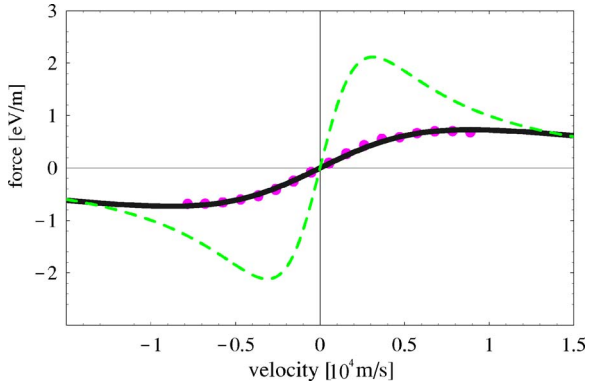

FIG. 8. (Color online) Longitudinal friction force in [eV/m] vs velocity [$\times10^4$ m/s] for electron current of 300 mA ($B=0.12$ T). Experimental data: dots; solid line (black): the force averaged according to Eq. (4) with fixed coefficient $C=1/\pi$ and fitted effective velocity 4000 m/s; dashed line (green): single-particle force according to the Eq. (3) with corresponding effective velocity 4000 m/s.

There could be different approaches to a fitting procedure based on averaging in Eq. (4). The first one assumes that the

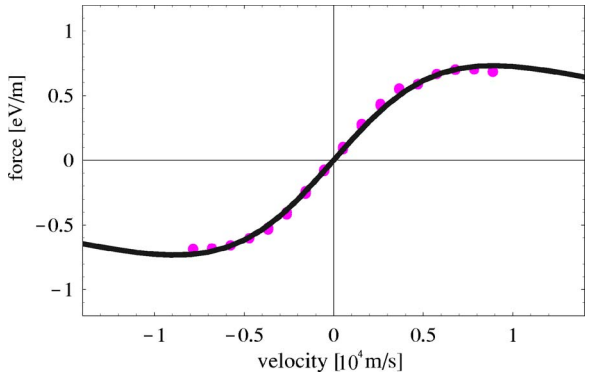

FIG. 9. (Color online) Measured force (dots) in [eV/m] vs velocity [$\times10^4$ m/s] for an electron current of 300 mA ($B=0.12$ T) and the fitting curve according to the Eq. (4) with an experimentally determined effective velocity.

numerical coefficient C in the expression for the single-particle force in Eq. (3) is known (for example, $C=1/\pi$ as in Ref. [18] or $C=1/\sqrt{2\pi}$ as in Ref. [19] for low relative velocities), while Δ_{eff} is a fitting parameter. In our experiments, the measured transverse rms velocity spread of the proton beam was rather large so that the fitted Δ_{eff}, as a result of such averaging, became very small ($\Delta_{eff}=4000$ m/s is needed for the case shown in Fig. 8). For such low value of the effective velocity, the single-particle friction force would have a maximum around this small value having a nonlinear decrease of the force for larger velocities. As a result, significant large-amplitude oscillations are expected for the relative velocities corresponding to the nonlinear part of the force [14]. However, we did not see such oscillations for the velocities in this range. In fact, we measured the maximum of the friction force by recording the onset of such large-amplitude oscillations which took place at significantly larger velocities.

The second approach is to take Δ_{eff} as a known parameter based on recorded oscillations of the longitudinal profile and the measured maximum of the friction force (see Sec. III). The fitting parameter is then the unknown numerical coefficient C. In such an approach (for our parameters and the region of low relative velocities discussed here), using the measured value of the velocity corresponding to the force maximum which is about 8000 m/s and Eq. (4), we find some enhancement for the numerical coefficient C compared to the factor $1/\pi$ [18]. For the fitting presented in Fig. 9 (solid line), the coefficient obtained is $C=1.6/\pi$. Note that an uncertainty of the numerical factor C found by such a procedure is rather large due to significant error bars in the measurements of the proton distribution and the uncertainty in the momentum spread value for the longitudinally space-charge dominated beam [21].

As a result, we can only say that with the convolution over the ion distribution (which we believe is the correct approach) the numerical factor C appears to be somewhat higher than $1/\pi$ [18], and, to the accuracy of the present analysis, seems to be in reasonable agreement with an analytic coefficient $C=1/\sqrt{2\pi}$ [19].

As discussed above, it appears rather difficult to extract a microscopic (single-particle) cooling force with very good accuracy from a macroscopic quantity of the measured phase shift. We plan to accurately determine numerical factors for the single-particle friction force expressions using numerical simulations with the VORPAL code and by studying the velocities of ions intercepting the magnetic field lines at an angle [10,22].

V. SUMMARY

In this paper, we report a series of dedicated measurements of the longitudinal magnetized friction force in CELSIUS. The goal of the measurements was to obtain data suitable for a detailed quantitative comparison with theoretical models and simulations. A high precision in the measurements was obtained due to a combination of the two effects: changing the rf frequency instead of the electron voltage and accurate measurements of the phase difference using a phase discriminator. The friction force was measured for various parameters of the cooler, including different currents of the electron beam, various strength of the magnetic field, different strength of the magnetic field errors in the cooling solenoid and the misalignment angle between the beams. We also discuss the procedure of fitting the experimental data with a parametric expression for the force, as well as some insights gained in our studies.

ACKNOWLEDGMENTS

We would like to thank Dag Reistad and the The Svedberg Laboratory for providing beam time and support during these experiments. We are grateful to Oliver Boine-Frankenheim and Ilan Ben-Zvi for taking an active role in planning these experiments, and for many useful discussions. We also thank Sergei Nagaitsev for helpful comments about the analysis of our experimental data. A. Sidorin, A. Smirnov, and V. Ziemann acknowledge the support from INTAS Grant No. 03-54-5584 "Advanced Beam Dynamics for Storage Rings." This work was supported by the U.S. Department of Energy.

[1] G. I. Budker, At. Energ. **22**, 346 (1967).
[2] V. V. Parkhomchuk and A. N. Skrinsky, Rep. Prog. Phys. **54**, 919 (1991).
[3] M. Larsson, Rep. Prog. Phys. **58**, 1267 (1995).
[4] I. Meshkov, Nucl. Instrum. Methods Phys. Res. A **391**, 1 (1997).
[5] C. Ekström *et al.*, Phys. Scr. **T22**, 256 (1988).
[6] M. Sedlaček *et al.*, *Proceedings of the Workshop on Cooling*, Montreux, Switzerland, October 1993, CERN 94-03, p. 235; details are provided in the report by M. Sedlaček *et al.*, "CELSIUS electron cooler design" (unpublished).
[7] H. Danared, Nucl. Instrum. Methods Phys. Res. A **391**, 24 (1997).
[8] N. S. Dikansky, V. I. Kudelainen, V. A. Lebedev, I. N. Meshkov, V. V. Parkhomchuk, A. A. Sery, A. N. Skrinsky, and B. N. Sukhina, BINP Tech Report 88-61, Institute of Nuclear Physics, Novosibirsk, Russia, 1988.
[9] T. Ellison, *Proceedings of the 1991 Particle Accelerator Conference, San Francisco, May 1991*, p. 1612.
[10] A. V. Fedotov, D. L. Bruhwiler, D. T. Abell, and A. O. Sidorin, AIP Conf. Proc. **821**, p. 319 (2006).
[11] RHIC Electron Cooling, http://www.bnl.gov.cad/ecooling
[12] FAIR facility, http://www.gsi.de/GSI-Future/cdr
[13] B. Gålnander *et al.*, in *Beam Cooling and Related Topics: International Workshop on Beam Cooling and Related Topics*, edited by S. Nagaitsev and R. J. Pasquinelli, AIP Conf. Proc. No. 821 (AIP, Melville, NY, 2006) p. 259.
[14] D. D. Caussyn *et al.*, Phys. Rev. E **51**, 4947 (1995).

[15] A. Burov, FNAL Tech Note TM-2213 (2003).
[16] G. Parzen, BNL Tech Note C-AD/AP/150 (2004).
[17] A. V. Fedotov *et al.*, *Proceedings of the 2005 Particle Accelerator Conference*, Knoxville, TN, May 2005, p. 4263.
[18] V. V. Parkhomchuk, Nucl. Instrum. Methods Phys. Res. A **441**, 9 (2000).
[19] Ya. Derbenev and A. Skrinsky, Part. Accel. **8**, 235 (1978); *Physics Reviews Ser. Sov. Phys. Rev.*, edited by I. M. Khalatnikov (Harwood Academic, 1981), p. 165.
[20] T. Ellison *et al.*, Phys. Rev. Lett. **70**, 790 (1993).
[21] S. Nagaitsev *et al.*, *Proceedings of the Workshop on Cooling*, Montreux, 1993, CERN94-03, p. 405.
[22] D. L. Bruhwiler *et al.*, *Proceedings of the 2005 Particle Accelerator Conference*, Knoxville, TN, May 2005, p. 4206.
[23] Lars Hermansson (private communication). For an estimate of the magnetic field errors we used the latest measurements for the cooling solenoid provided by L. Hermansson (unpublished).